

Bias voltage and temperature dependence of magneto-electric properties in double-barrier magnetic tunnel junction with amorphous Co-Fe-B electrodes

Z.M. Zeng^{1,a}, Y. Wang¹, X.F. Han¹, W.S. Zhan¹, and Z. Zhang²

¹ National Laboratory for Condensed Matter Physics, Institute of Physics, Chinese Academy of Science, Beijing 100080, P.R. China

² Beijing University of Technology, Beijing 100022, P.R. China

Received 17 January 2006 / Received in final form 15 May 2006

Published online 31 July 2006 – © EDP Sciences, Società Italiana di Fisica, Springer-Verlag 2006

Abstract. Bias voltage and temperature dependence of magneto-electric properties in double-barrier magnetic tunnel junctions (DBMTJs) with a structure of [IrMn/CoFe/Ru/CoFeB]/Al-O/CoFeB/Al-O/[CoFeB/Ru/CoFe/IrMn], have been investigated. The DBMTJs show a large tunnel magnetoresistance (TMR) ratio of up to 57.6%, a high $V_{1/2}$ value of 1.26 V and small switching field H_c of 9.5 Oe at room temperature (RT). The TMR reaches the maximum at 30 K, about 89.0%, and decreases slightly from 30 to 4.2 K. A novel zero-bias anomaly (ZBA) in the P state is found and is temperature dependent, more sharply at low temperature, whereas a normal ZBA exists in the AP state. These effects are ascribed to magnon-, phonon- and impurity-assisted tunneling, and variation of density of states. The DBMTJ with a large TMR ratio, a high $V_{1/2}$, and small switching field H_c is promising for developing the future spin electronic devices.

PACS. 73.43.Qt Magnetoresistance – 75.47.-m Magnetotransport phenomena; materials for magnetotransport – 85.75.-d Magnetoelectronics; spintronics: devices exploiting spin polarized transport or integrated magnetic fields

1 Introduction

Recently spin dependent transport has received much attention due to its promising perspectives for applications, such as magnetic random access memories (MRAMs), magnetic read heads, and magnetic sensors since the discovery of the large tunneling magnetoresistance (TMR) effect at room temperature (RT) observed in magnetic tunnel junction (MTJ) [1,2]. Many attempts to improve the quality of MTJ have been made by (1) improving interface morphology between the barrier and electrodes, (2) optimizing barrier oxidation conditions and (3) using various ferromagnetic (FM) materials with large spin polarization, e.g., Wang et al. [3] have achieved the TMR ratio of about 70% using a Co-Fe-B alloys as the FM layers. Parkin et al. [4] and Yuasa et al. [5] have independently reported considerably large TMR ratio over 100% in MgO-based MTJs. However, the TMR value is strongly reduced when the applied bias voltage is of the order of a few hundred millivolts [2,6]. Up to now, the best value of $V_{1/2}$ in single barrier MTJ, at which the zero bias TMR value is halved, is less than 700 mV in the reported literatures [7,8].

The double-barrier magnetic tunnel junction (DBMTJ) has drawn increasingly attention from the physical and the application point of view due to its several advantages over single barrier MTJ (SBMTJ): (1) a higher TMR value shown in theoretical work [9]; (2) be suitable for investigating the spin-polarized electron coherent tunneling [10]; and (3) TMR of DBMTJ decreases more slowly than that of SBMTJ as a function of the bias voltage and has a higher $V_{1/2}$ value [11–14]. However, only a few experiments on the DBMTJs are reported due to the difficulties related to the upper barrier preparation. Colis et al. [12] reported the TMR ratio of 49.5% and $V_{1/2}$ of 1.33 V in DBMTJs with Co-Fe electrodes, but they showed a comparatively large switching field of free layer for application. Recently Nozaki et al. [14] found the TMR of 110% and $V_{1/2}$ of 1.44 V at positive bias voltage in a fully epitaxial Fe(001)/MgO(001)/Fe(001)/MgO(001)/Fe(001) structure, however, it showed large asymmetry in bias voltage dependence of TMR ratio, and the value of the $V_{1/2}$ at negative bias voltage is only 0.72 V. Such large asymmetry probably limits the application of the future spin electronic devices. Furthermore, the fully epitaxial method is not easy to commercialize due to comparatively high cost in the practical product. The

^a e-mail: zzm0167@aphy.iphy.ac.cn

reported results show the Co-Fe-B alloys have large spin polarization [3,15], and there are no literatures about magneto-electric properties in DBMTJs with amorphous Co-Fe-B electrodes. In this work, we investigate the bias voltage and temperature dependence of magneto-electric properties in the DBMTJ with amorphous Co-Fe-B electrodes.

2 Experimental

In this work, we fabricated the DBMTJs with an architecture of Si/SiO₂/Ru(5)/Ni₇₉Fe₂₁(5)/Ir₂₂Mn₇₈(12)/Co₇₅Fe₂₅(4)/Ru(0.8)/Co₆₀Fe₂₀B₂₀(4)/Al(1.3)-oxide/Co₆₀Fe₂₀B₂₀(4)/Al(1.3)-oxide/Co₆₀Fe₂₀B₂₀(4)/Ru(0.8)/Co₇₅Fe₂₅(4)/Ir₂₂-Mn₇₈(12)/Ni₇₉Fe₂₁(5)/Ru(5), where the numbers in parentheses have a unit of nanometer. The multilayer were deposited using an ULVAC TMR R&D Magnetron Sputtering System (MPS-4000-HC7) with a base pressure of below 5×10^{-7} Pa. During the deposition, magnetic field of about 100 Oe was applied to define the uniaxial magnetic anisotropy of the magnetic layer. Al-oxide layers were formed by plasma oxidization of 1.3 nm Al at 1 Pa for 70 s at a separate chamber. The elliptic junctions with an area of $\pi \times 4 \times 12 \mu\text{m}^2$ were patterned using the conventional photolithography combined Ar ion-beam etching and lift-off techniques. All processes were done in the clean room. The magnetic transport properties of the DBMTJs were measured using dc four-probe method with the Physical Properties Measurement System (PPMS) after annealing at 548 K for an hour to improve the morphology of the layer surface.

3 Results and discussions

Figure 1 shows a cross-sectional transmission electron microscopy (TEM) image in which the layers of the DBMTJ with amorphous Co-Fe-B electrodes can be clearly distinguished. Two continuous white lines in the middle are Al-O layers, which indicates that two Al-O tunnel barriers are continuous on a large scale. A high resolution TEM (HRTEM) image is shown in Figure 1b, which gives a magnified and clear view of the middle layers in the box area in Figure 1a. Amorphous Al-O layers are observed and the thicknesses of the top and bottom barrier layer are estimated to be between 1.3 and 1.7 nm. The top, middle and bottom Co-Fe-B layers show an amorphous structure.

Figure 2 shows the TMR curves of a typical DBMTJ under the constant bias voltage application of $V = +5$ mV at several temperatures (300, 150, 77, 30, and 4.2 K) TMR ratio is defined as $\text{TMR} = (R_{AP} - R_P) / R_P$, where R_{AP} and R_P denote the tunnel resistance when the magnetization of the free layer versus two pinned magnetic electrodes are aligned anti-parallel (AP) and parallel (P) configurations, respectively. We observe the TMR ratio of up to 57.6% and 89% for the DBMTJ with the resistance area

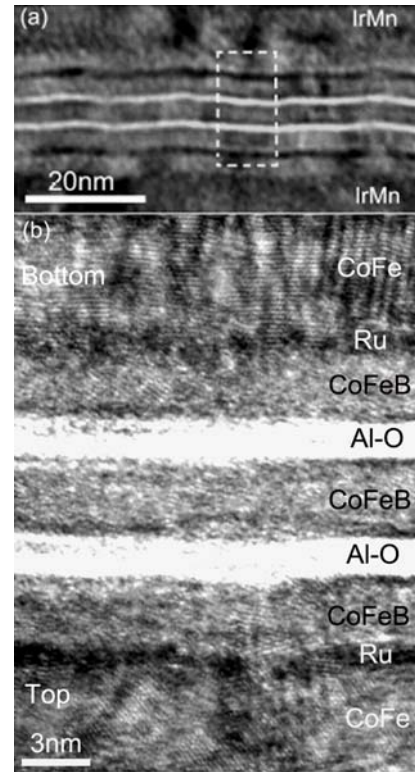


Fig. 1. A cross-sectional TEM image of a typical DBMTJ and Figure 1b is the magnified image of the square part as shown in Figure 1a.

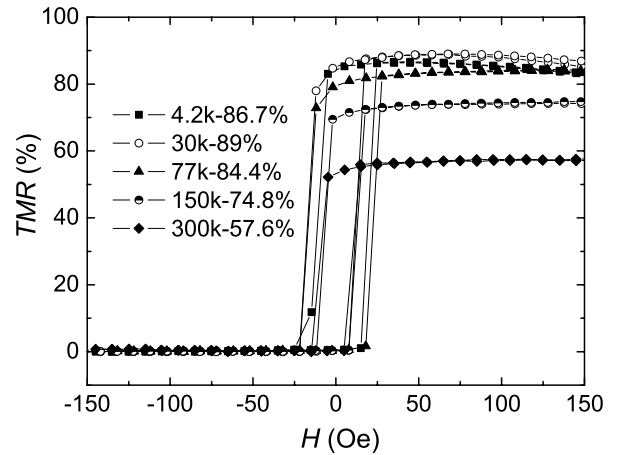


Fig. 2. TMR curves of a typical DBMTJ at several temperatures (300, 150, 77, 30 and 4.2 K) under the constant bias voltage application of $V = +5$ mV.

product (RA) of 11.6 and 12.5 $\text{k}\Omega \mu\text{m}^2$ at RT and 30 K, respectively, which is the highest TMR ratio using magnetron sputtering methods ever reported for the DBMTJs, higher than that in reference [12]. The switching field (H_c) of the middle free layer of the DBMTJs is about 9.5 Oe at RT and 14 Oe at 30 K. These experimental results show that the DBMTJ with Co-Fe-B electrodes is a candidate for developing the future spin electronic devices.

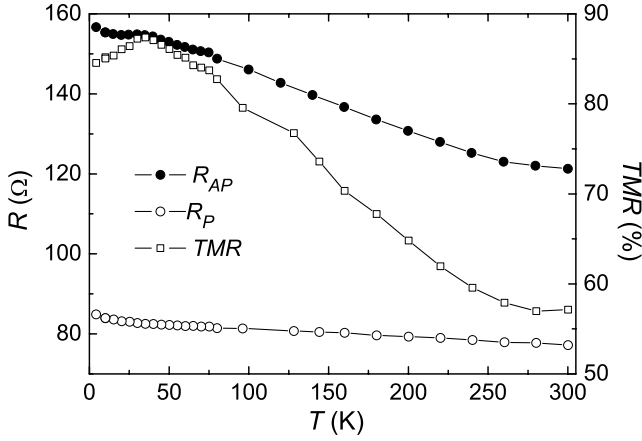


Fig. 3. Temperature dependence of the TMR ratio and junction resistance for the same DBMTJ.

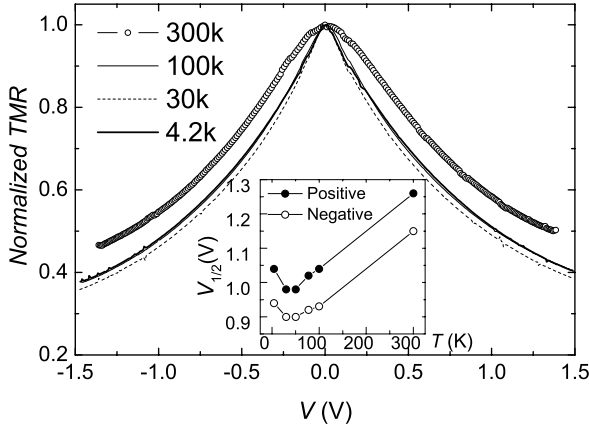


Fig. 4. Bias voltage dependence of the TMR for the same DBMTJ at several temperatures. The inset shows the temperature dependence of the $V_{1/2}$.

We also investigate the bias voltage and temperature dependence of magneto-electric properties. Figure 3 shows the temperature dependence of the TMR ratio and resistances from 4.2 K to RT. The magnetic fields of ± 100 Oe were applied to set the magnetization state of the junction in the *AP* and *P* states, respectively. It can be seen that the resistance R_{AP} of the *AP* state increases rapidly with decreasing the temperature, whereas the resistance R_P for the *P* state hardly changes at all on cooling, which results in the TMR ratio increase with decreasing the temperature. A maximum TMR ratio of 89% was observed at 30 K, which increased 54.5% compared with that of 57.6% at RT due to the decrease of magnon and phonon excitations [16]. The TMR ratio decreased slightly below 30 K is due to: (1) the decrease of the spin polarization which is due to the thermal excitation of spin waves [17] and the spin-glass-like states at the interfaces between the free layer and the insulating layer [18]; (2) the anti-parallel alignment of magnetization was incomplete due to the the

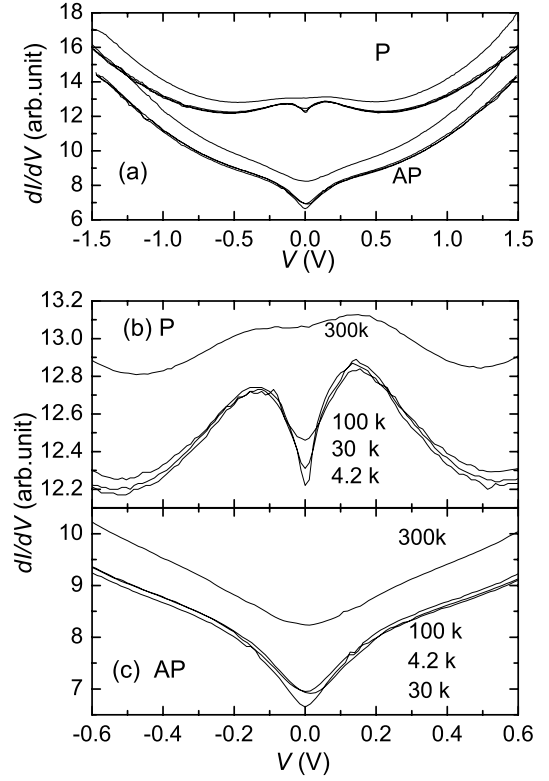


Fig. 5. *AP* and *P* dynamic conductance at several temperatures (4.2, 30, 100, and 300 K).

increased coercivity of the middle ferromagnetic free layer with decreasing temperature.

There is slightly asymmetric bias voltage dependence in DBMTJs with amorphous Co-Fe-B electrodes as shown in Figure 4, which has been also observed in other literatures. Such asymmetry is due to the subtle differences in Co-Fe-B/Al-O interfaces. It also shows the $V_{1/2}$ of +1.26 and -1.19 V for positive and negative bias at RT, respectively, where the polarity of the bias voltage is defined as positive when the current flows from the top to the bottom layers of the DBMTJs. The $V_{1/2}$ enhancement is produced by the reduction of the effective bias voltage applied to the individual two barriers. And the bias dependence of TMR is also temperature dependent, the $V_{1/2}$ decreases with decreasing temperature from 300 to 30 K, then increases slightly from 30 to 4.2 K as shown in inset graph of Figure 4.

We further investigate the conductance (junction resistance) as a function of applied bias voltage at low temperature. $I-V$ curves were measured under the *AP* state and *P* state at several different temperatures, and both *AP* and *P* configurations were measured at ± 100 Oe, respectively. $G(V)$ [$G = dI/dV$] curves were obtained by Lock-in technology, an ac modulation voltage of 2.0 mV with a frequency of 6.8 kHz was applied to the junction. Figure 5 shows the bias voltage dependence of the conductance for both *P* and *AP* states at several temperatures (see Fig. 5a). It can be seen that the G (resistance) for

AP state ascends (drops) as the applied voltage increases, the G increases with temperature rather significantly (see Fig. 5c), where the resistance versus the bias is not shown. We notice a rapid increment in the G of the junction with a width of about 130 mV; we have called this the “zero bias anomaly” (ZBA). Whereas the G for the *P* state has novel zero-bias anomaly phenomenon, the main features is: (1) the G increases rapidly at zero bias voltage from 0 to 0.13 V; (2) the G decreases at range from 0.13 to 0.53 V; (3) the G increases again with increasing at high bias voltage (>0.53 V) as shown in Figure 5b. This effect is also temperature dependent, with the peak being more sharply at low temperature. The origin of this effect is still elusive. We propose that this effect may involve the magnon- and phonon- scattering, impurity scattering and variety of density of states. The increase of the conductance at less than 100 mV for the *AP* and *P* states is ascribed to inelastic magnon-assisted tunneling [19,20] and impurity-assisted tunneling [21]. While the change at 150–500 mV is due to phonon assisted tunneling [21], and the change at high voltage (>500 mV) is relative to variations of the density of states [24]. A much refined theory is needed in order to quantitatively explain this effect.

4 Summary

In summary, we have fabricated DBMTJs with amorphous Co-Fe-B electrodes by using magnetron sputtering and micro-fabrication technique, and investigated the bias voltage and temperature dependence of magneto-electric properties. A novel ZBA is found in the *P* state and is temperature dependent, more sharply at low temperature, which is ascribed to magnon-, phonon- and impurity-assisted tunneling and variation of the density of the states. The DBMTJs show a large TMR ratio of 57.6%, $V_{1/2}$ of 1.26 V and H_c of 9.5 Oe at RT. These experimental results show the Co-Fe-B based DBMTJ is promising for developing the spin-polarization devices.

The project was supported by the State Key Project of Fundamental Research of Ministry of Science and Technology Grant No. 2001CB610601 and 2002CB613500, China. X.F.H. gratefully thanks the partial support of Distinct Researcher Foundation (50325104) and Chinese National Natural Science Foundation (10274103, 50271081).

References

1. T. Miyazaki, N. Tezuka, J. Magn. Magn. Mater. **81**, L231 (1995)
2. J.S. Moodera, L.R. Kinder, T.M. Wong, R. Meservey, Phys. Rev. Lett. **74**, 3273 (1995)
3. D. Wang, C. Nordman, J.M. Daughton, Z. Qian, J. Fing, IEEE Trans. Magn. **40**, 2269 (2004)
4. S.S. Parkin, C. Kaiser, A. Panchula, P.M. Rice, B. Hughes, M. Samant, S.-H. Yang, Nature Mater. **3**, 862 (2004)
5. S. Yuasa, T. Nagahama, A. Fukushima, Y. Suzuki, K. Ando, Nature Mater. **3**, 868 (2004)
6. A.C. Marley, S.S.P. Parkin, J. Appl. Phys. **81**, 5526 (1997); W.J. Gallagher, J. Appl. Phys. **81**, 3741 (1997)
7. S.-J. Ahn, T. Kato, H. Kubota, Y. Ando, T. Miyazaki, Appl. Phys. Lett. **86**, 102506 (2005)
8. D.D. Djayaprawira, K. Tsunekawa, M. Nagai, H. Maehara, S. Yamagata, N. Watanabe, S. Yuasa, Y. Suzuki, K. Ando, Appl. Phys. Lett. **86**, 92502 (2005)
9. X. Zhang, B.-Z. Li, G. Sun, F.-C. Pu, Phys. Rev. B **56**, 5484 (1997)
10. S. Stein, R. Schmitz, H. Kohlstedt, Solid State Communications **117**, 599 (2001)
11. F. Montaigne, J. Nassar, A. Vaurés, F. Nguyen Van Dau, F. Petroff, A. Schuhl, A. Fert, Appl. Phys. Lett. **73**, 2829 (1997)
12. S. Colis, G. Gieres, L. Bär, J. Wecker, Appl. Phys. Lett. **83**, 948 (2003)
13. X.F. Han, S.F. Zhao, F.F. Li, T. Daibou, H. Kubota, Y. Ando, T. Miyazaki, J. Magn. Magn. Mater. **282**, 225 (2004)
14. T. Nozaki, A. Hirohata, N. Tezuka, S. Sugimoto, K. Inomata, Appl. Phys. Lett. **86**, 82501 (2005)
15. F.F. Li, X.F. Han, L.X. Jiang, J. Zhao, L. Wang, R. Sharif, J. Mater. Sci. Tech. **21**, 289 (2005)
16. X.F. Han, M. Oogane, H. Kubota, Y. Ando, T. Miyazaki, Appl. Phys. Lett. **77**, 283 (2000)
17. C.H. Shang, J. Nowak, R. Jansen, J.S. Moodera, Phys. Rev. B **58**, R2917 (1998)
18. L. Yuan, S.H. Liou, Wexin wang, Phys. Rev. B **73**, 134403 (2006)
19. S. Zhang, P.M. Levy, A.C. Marley, S.S.P. Parkin, Phys. Rev. Lett. **79**, 3744 (1997)
20. Edward McCann, Vladimir I. Falco, Phys. Rev. B **66**, 134424 (2002); Appl. Phys. Lett. **81**, 3609 (2002)
21. A.M. Bratkovsky, Appl. Phys. Lett. **72**, 2334 (1998); Phys. Rev. B **56**, 2344 (1997)
22. X.F. Han, J. Murai, Y. Ando, H. Kubota, T. Miyazaki, Appl. Phys. Lett. **78**, 2533 (2001)
23. C. Lü, M.W. Wu, X.F. Han, Phys. Lett. A **319**, 205 (2003)
24. G.G. Cabrera, N. García, Appl. Phys. Lett. **80**, 1782 (2002)